Shedding light on precursor and thermal treatment effects on the nanostructure of electrospun TiO2 fibers

Published version:

DOI:10.1016/j.nanoso.2016.05.003

Shedding light on precursor and thermal treatment effects on the nanostructure of electrospun TiO_2 fibers

Sara Morandi, Claudio Cecone, Giulia Marchisio, Pierangiola Bracco, Marco Zanetti and Maela Manzoli*

Dipartimento di Chimica,Università di Torino and NIS, Interdepartmental Centre, Via P. Giuria 7, 10125 Torino, Italy.

***Corresponding author**: Dr. Maela Manzoli, phone: +390116707541, e-mail: maela.manzoli@unito.it

Abstract

Electrospinning technique was employed for the synthesis of different TiO_2 samples, starting from titanium oxysulfate and titanium n-butoxide (TNBT) as precursors. The electrospun fibers, obtained after optimization of starting solutions, were either calcined in air at 450 °C or treated in 50 mbar of pure oxygen at 450 °C. The main goal was to obtain TiO_2 fibers constituted by crystallites with size lower than 10 nm (size largely reported in literature for this kind of synthesis) in the anatase form. Before thermal treatment, the morphology of the fibers was characterized by Scanning Electron Microscopy (SEM); after thermal treatment TiO_2 morphological and structural properties were determined by Transmission Electron Microscopy (TEM) as well as by high resolution (HR-) TEM and X-Ray Diffraction (XRD).

TiO_2 prepared with TNBT precursor and treated in oxygen at 450 °C gave the best results in terms of crystalline phase (pure anatase) and particle size (about 5 nm). Moreover, HR-TEM analysis of the fibers obtained from TNBT before thermal treatment revealed that the precursor crystallization occurred already at room temperature during the electrospinning process, giving rise to nucleation germs for the subsequent growth of TiO_2 crystallites during the thermal treatment. On the contrary, samples prepared by electrospray and by simple solvent evaporation at room temperature of the solution with the same TNBT precursor did not give the same promising results in terms of crystalline phase and particle size.

Keywords: Electrospinning, titanium oxysulfate, titanium n-butoxide, TiO_2, HR-TEM

1. Introduction

Titanium dioxide (TiO_2) is a versatile transition-metal oxide, widely investigated as a useful material in a wide range of applications including solar cells [1, 2], photocatalysts for air and water purification [3-5], gas sensors [6-8] and biocompatible coatings for biomaterials [9, 10]. The most common crystalline forms of TiO_2 are anatase and rutile, both showing a tetragonal crystalline structure. For the solar cell and photo-catalysis applications, only the anatase TiO_2 exhibits high activity. However, the high rate of recombination of photo-induced electron and hole pairs limits its photo-activity, which strongly depends on physico-chemical parameters such as particle size and surface area as well as overall morphology. To further improve the properties of TiO_2 and to expand potential applications, low-dimensional nanostructures with controllable crystalline phases, such as nanoparticles, nanofibers, nanostructured thin films or coatings and nanotubes have been extensively studied. In particular, TiO_2 microtubes constituted by defined nanoscale particles have attracted considerable attention [11-16].

Electrospinning represents a relatively simple and versatile method for generating porous fiber mats with interconnective pores and high specific area [17]. In a typical process, a polymer solution or melt is injected from a small noozle under the influence of an electric field as strong as several kV/cm. The built up of electrostatic charges on the surface of a liquid droplet induces the formation of a jet, which is subsequently stretched to form a continuous ultrathin fiber. In the continuous-feeding mode, numerous copies of fibers can be formed within a period of time as short as a few seconds.

Until the early 2000s, electrospinning was mainly applied to pure organic polymers. In the last fifteen years, electrospinning of solutions containing precursors of ceramics followed by high temperature pyrolysis was adopted to obtain ceramic nanofibers [18-21]. In particular, in the last few years, electrospinning synthesis of titania have demonstrated that the fibers obtained after calcination are poly-crystalline with crystallite size in the range 10-50 nm [12, 13, 15, 22-25].

In the present work, different precursors and different thermal treatments on electrospun fibers were tested to obtain poly-crystalline TiO_2 fibers with crystallite size lower than 10 nm in the anatase form. Before thermal treatment, the morphology of the fibers was characterized by Scanning Electron Microscopy (SEM); after thermal treatment TiO_2 morphological and structural properties were determined by Transmission Electron Microscopy (TEM) and High Resolution Transmission Electron Microscopy (HR-TEM) as well as by X-Ray Diffraction (XRD).

2. Experimental

2.1. Synthesis of the samples

Solutions for electrospinning were prepared using titanium(IV) oxysulfate ($TiOSO_4$, Sigma-Aldrich) or titanium (IV) n-butoxide (TNBT, Sigma-Aldrich) as precursors. In the first case, an aqueous solution containing polyvinylpyrrolidone (PVP, 1300000 uma, Sigma-Aldrich) and $TiOSO_4$ precursor was prepared and loaded into a syringe equipped with a BD Precisionglige needle (size 27 gauge) made of stainless steel and connected to a high voltage supply (GLASSMAN High Voltage, EL) capable of generating DC voltages up to 30 kV. As-electrospun fibers were collected on a drum collector (length: 120 mm, diameter: 80 mm), covered with an aluminum foil. During electrospinning, a positive voltage of 30 kV was applied between the needle and the collector with a working distance of 14 cm. The feeding rate for the polymer-precursor solution was controlled using a syringe pump (Biological Instruments, KD Scientific) and was set at 2 μl/min. The electrospinning process was conducted in air at room temperature (RT). PVP and $TiOSO_4$ concentrations were optimized in order to obtain well defined fibrous structure as evidenced by SEM analysis (vide infra). Based on the results of a previous screening, PVP concentrations between 13 and 25% and PVP/$TiOSO_4$ weight ratio ranging between 2/1 and 3/1 were tested, as reported in Table 1.

Table 1. List of the solutions used for the optimization of the electrospinning process with $TiOSO_4$ precursor.

Solution n°	**1**	**2**	**3**	**4**	**5**	**6**	**7**
PVP wt.%	13	14	15	18	20	22	25
PVP/$TiOSO_4$ (w/w)	2/1	2.5/1	3/1	3/1	3/1	3/1	3/1

As for the TNBT precursor, a solution was prepared by mixing two parts of ethanol, one part of TNBT and two parts of acetic acid, which is added to stabilize the solution by controlling the hydrolysis reactions of the sol-gel precursor [11, 26]. A second solution with PVP (1300000 uma) in ethanol was prepared. Also in this case the PVP concentration was optimized by checking the solutions reported in Table 2 in order to obtain well defined fibrous structure as evidenced by SEM analysis (vide infra).

Table 2. List of the solutions used for the optimization of the electrospinning process with TNBT precursor.

Solution n°	**1**	**2**	**3**	**4**	**5**
PVP wt.%	7	10	15	18	20

Equal volumes of the two solutions were mixed just before the loading in the syringe for the electrospinning process, in air, at RT with a feeding rate of 10 μl/min, a voltage of 30 kV and a working distance of 14 cm.

For each precursor only the sample with the best fiber morphology underwent two different thermal treatments to burn the organic component: (i) calcination in air at 450 °C for 3 hours; (ii) thermal treatment in 50 mbar of pure oxygen at 450 °C for 5 hours, changing oxygen every hour. In this way four TiO_2 samples were prepared: two with $TiOSO_4$ precursor, named TiOSair (calcination in air) and TiOSOx (thermal treatment in O_2), and two with TNBT precursor, named TNBTair (calcination in air) and TNBTOx (thermal treatment in O_2).

For comparison purposes, the solution containing TNBT precursor was also used for preparing samples by electrospray technique and by simple evaporation of the solvent at RT. To prepare the sample by electrospray technique the same apparatus employed for the electrospinning procedure was used. In this case, PVP with a lower molecular weight (30000 uma) was used in order to obtain droplets instead of fibers.

2.2. Characterization techniques

Thermo-gravimetric analysis (TGA) of the electro-spun samples was performed by a TGA Q500 TAInstrument, using a temperature ramp of 10 °C/min up to 800 °C in air.

Morphological characterization of the samples was performed by: (i) Scanning Electron Microscopy (SEM) using a Leica Stereoscan 410 microscope (Oxford Instruments), operating at 15 kV. All the polymer-containing samples were gold sputtered prior to examination; (ii) Transmission Electron Microscopy (TEM) and High Resolution (HR)-TEM using a side entry Jeol JEM 3010 (300 kV) microscope equipped with a LaB_6 filament. For analyses, if not differently specified, the synthesized samples were deposited on a copper grid, coated with a porous carbon film. All digital micrographs were acquired by an Ultrascan 1000 camera and the images were processed by Gatan digital micrograph. A statistically representative number of crystallites was counted in order to obtain the particle size distribution, where the mean particle diameter (d_m) was calculated as $d_m = \Sigma d_i n_i / \Sigma n_i$, where n_i was the number of particles of diameter d_i.

Structural characterization of the samples after thermal treatment was carried out on an Oxford Diffraction Gemini-R Ultra diffractometer (Cu-Kα radiation, λ=1.5418 Å) equipped with an Enhanced Ultra collimator, a four-circle Kappa geometry goniometer and a RUBY CCD collector. This instrument, suitable for XRD measurement on single crystals, was adapted to work with powders: the advantage is the very low amount of sample necessary for an accurate measure. The crystallite size of TiO_2 was calculated by applying the Scherrer's formula using the (101) diffraction peak for anatase and the (110) diffraction peak for rutile in the XRD patterns.

3. Results and Discussion

3.1 Fiber synthesis optimization

The purpose of this work has been to use a polymer as template for the production of titania nanoparticles. With this aim we selected PVP as the base polymer because of its good solubility in alcohols and water and because of its compatibility with both organic and inorganic titania precursors even when its molecular weight is as high as 1300000 uma.

In Figure 1 SEM images of the as prepared samples obtained by electrospinning of solutions with $TiOSO_4$ precursor are shown. Solutions 1, 2 and 3 (see Table 1) give the same morphology, which is reported in Fig.1A for solution 2: an high amount of beads is observed, indicating a too low solution viscosity. Images in section B and C related to the electrospinning of solutions 4 and 5, respectively, show the presence of quite defined fibers, even if some fiber adhesion is still present. Solutions 6 and 7 allow to obtain well defined fibers as reported in image of section D for solution 7. This last sample was chosen for the subsequent thermal treatments in air and in pure oxygen at 450 °C for obtaining TiO_2 specimens.

In Figure 2 SEM images of the as prepared samples obtained by electrospinning of solutions with TNBT precursor are shown. The results obtained with solutions 1 and 2 (see Table 2) is the same and is reported in section A for solution 2: the presence of beads enlightens the too low viscosity of the solution. The increase of PVP concentration increases the solution viscosity, causing the decrease of beads amount with solution 3 (image in section B) and their disappearance with solutions 4 and 5 (see image in section C related to solution 5). The sample with well defined fibers obtained with solution 5 was chosen for the subsequent thermal treatments.

It is worth of note that with $TiOSO_4$ precursor the best obtained fibers (Fig. 1D) are wider (the diameters have size in the range between 1.5 μm and 7.0 μm) than in the case of TNBT precursor, that guaranteed fibers with homogeneous diameter < 1.0 μm (Fig. 2C). This is likely due to differences in viscosity and conductivity between the two precursor solutions.

The TG analysis performed in air on the two samples chosen for undergoing thermal treatments shows that for both of them the weight loss associated to the polymer volatilization ends at about 450 °C (Figure 3). For this reason, the temperature of 450 °C was chosen for carrying out calcination and thermal treatment in 50 mbar of pure oxygen.

3.2 Characterization of TiO_2 samples obtained by electrospinning

After thermal treatments four samples were obtained: TiOSair, TiOSOx, TNBTair and TNBTOx, whose diffraction patterns are reported in Figure 4. TiOSair is constituted mainly by anatase with small amount of rutile phase (curve a). The mean crystallite size of anatase is calculated to be about 11 nm. The diffraction pattern of TiOSOx (curve b) reveals a very low crystallinity of the sample with the presence of a very broad and weak peak at 25.3° related to the main (101) reflection of anatase. Moreover, at angles lower than 20° a very broad peak assignable to an amorphous phase is detected. As a matter of fact, the TiOSOx sample appears black, revealing the presence of a significant amount of carbonaceous residues. This result puts in evidence that the thermal treatment at 450 °C with low O_2 pressure is not sufficient to efficiently burn the organic component when using $TiOSO_4$ as precursor. With thermal treatments in pure oxygen at higher temperatures a relevant amount of rutile is obtained. This phase is undesired for photo-catalysis and solar cell applications.

As for samples prepared with TNBT precursor, the diffraction pattern of TNBTair (Fig. 4, curve c) shows the presence of both anatase and rutile phases. The mean crystallite size of anatase (using the (101) peak at 25.3°) and rutile (using the (110) peak at 27.4°) is calculated to be about 11 and 14 nm, respectively. The pattern of TNBTOx (Fig. 4, curve d) reveals a particularly interesting sample, constituted by only anatase with a mean crystallite size of about 5 nm.

TEM and HR-TEM measurements were performed on this last sample and two representative images are reported in Figure 5 sections A and B. The images reveal that the fibrous nature of the sample is maintained after the thermal treatment even if the fibers appear fragmented due to the lower mechanical resistance of the oxide with respect to the as-electrospun material. The analysis of the fiber diameter distribution, obtained by sampling 54 fibers, is reported in Figure 6A: the range of fiber diameter is 30-230 nm with a mean value of 79.0 nm and a standard deviation of 50.2 nm, evidencing a the presence of fibers with different diameter. However, it is well evident that the TiO_2 fibers are constituted by nano-particles whose crystalline nature is enlightened by diffraction fringes present in the HR-TEM image (Figure 5B) and by diffraction spots in the Fourier Transform of the image (Figure 5C). The analysis put in evidence spacing of 3.52, 2.37 and 1.88 nm related to the (101), (103) and (200) planes of tetragonal anatase (00-001-0562).

Particle size distribution, obtained by sampling 250 particles, is reported in Figure 6B. The sample is highly homogeneous, being the size distribution narrow with an average diameter (d_m) of 5.4 nm and a standard deviation of 1.1 nm, in full agreement with the result obtained on the basis of the XRD pattern.

It is worth of note that differently from the case of $TiOSO_4$, the thermal treatment in low oxygen pressure of the sample obtained from TNBT precursor allows to burn all the organic fraction already at 450 °C, obtaining pure anatase with particularly small particle sizes. Indeed, PVP is thermally degraded, predominantly, by the release of the pyrrolidone side group and the subsequent decomposition of polyenic sequences [27]. In inert atmosphere those polyenic sequences, undergoing to condensation reaction, may lead to the formation of a certain amount of carbonaceous residue. However, if the degradation is carried out in the presence of oxygen, the residue volatilizes completely through a thermo-oxidative mechanism. Results show that this reaction occur obviously in the case of TiOSAir and TNBTair, where the amount of oxygen is sufficient to produce the complete volatilization of the organic fraction at 450 °C. This also happens in the case of TNBTOx, where despite the low partial pressure of O_2 the volatilization of the organic phase is complete. However, in the case of TiOSOx the formation of a carbonaceous residue prevails. It must be considered that inorganic salts and acids are known to increase the char yields of degrading polymers, promoting dehydration reactions [28]. The presence of an acid salt like $TiOSO_4$ may enhance the formation of char at the point that it is impossible to be thermo-oxidized in the low-pressure condition employed.

In order to deepen the comprehension of the mechanism for the formation of TiO_2 nano-particles, HR-TEM analysis of the fibers before the thermal treatment was performed. For this purpose, fiber deposition was performed directly on a TEM copper grid. In Figure 7 an image of the not calcined fibers directly electrospun on the grid is shown. The related Fourier Transform is also reported as inset. Even if the sample has mainly an amorphous nature, some crystalline regions are present, as confirmed by the spots detected in the Fourier Transform of the acquired images. The distances of these spots from the transmitted beam can be related to sub-stoichiometric TiO_2 phases, such as Ti_2O_3 (JCPDS 00-010-0063), Ti_3O_5 (JCPDS 00-011-0217) and Ti_7O_{13} (JCPDS 00-018-1403). It is necessary to underline that the sample is stable under the electron beam, excluding the hypothesis of the formation of sub-stoichiometric TiO_2 phases during the HR-TEM analysis. This finding is of pivotal importance because evidence that the precursor crystallization occurs already at RT during the electrospinning process is given. The early crystallization can provide nucleation germs for the subsequent growth of TiO_2 crystallites during the thermal treatment in oxygen. This phenomenon, which is generally not observed when using other preparation techniques, might be favored by the stretching effect to which the precursor solution is usually subjected during electrospinning. Reasonably, the formation of a high amount of nucleation germs, as evidenced by HR-TEM measurements, along with low oxygen pressure can justify the formation of particles smaller than those obtained in the other cases under study.

3.3 Samples prepared by electrospray and solvent evaporation

In order to demonstrate the uniqueness of the electrospinning technique for obtaining TiO_2 with very small crystallite size in anatase form, other two samples were prepared by electrospray technique and by simple solvent evaporation at RT using the solution 5 of Table 2. It should be considered that in order to obtain droplets with electrospray, a lower molecular weight PVP (30.000 uma) was employed. In Figure 8 SEM image of the sample prepared by electrospray is reported, evidencing the formation of droplets in a wide range of diameters (0.1 - 2 μm).

The samples prepared by electrospray and solvent evaporation were treated at 450 °C in 50 mbar of oxygen, i.e. the thermal treatment that allowed to obtain the best TiO_2 sample in terms of crystalline phase (pure anatase) and particle size (about 5 nm) by electrospinning. However, for these two samples the thermal treatment was not sufficient to burn the entire organic fraction. In these last two cases, the samples have a lower specific area rendering more difficult the oxidation process, as much of the organic fraction to be ablate is located in the bulk in which the oxygen must diffuse. In order to obtain white sample, it was necessary to treat the electrospray sample at 650 °C and that obtained by simple solvent evaporation at 700 °C. This causes the formation of high amount of rutile phase with crystallite size of about 20 nm, as evidenced by XRD patterns reported in Figure 9.

4. Conclusions

In the present work, poly-crystalline TiO_2 fibers were synthesized through electrospinning technique. In particular, titanium(IV) oxysulfate ($TiOSO_4$) and titanium(IV) n-butoxide (TNBT) were used as precursors along with polyvinylpyrrolidone (PVP) for preparing solutions for electrospinning. Precursors and PVP concentrations were optimized to obtain well defined fibers. Both calcination in air and thermal treatment in 50 mbar of pure oxygen at 450 °C were performed for obtaining TiO_2 samples.

Among the synthesized TiO_2 samples, that prepared with TNBT precursor and treated in low oxygen pressure at 450 °C gives the best results in terms of crystalline phase and particle size: XRD pattern shows the presence of only anatase with a mean crystallite size of about 5 nm, in agreement with HR-TEM measurements. In particular, HR-TEM analysis of the fibers obtained from TNBT before thermal treatment puts in evidence that the precursor crystallization occurs already at RT during the electrospinning process, giving nucleation germs for the subsequent growth of TiO_2 crystallites during the thermal treatment. It is worth of note that the treatment in low oxygen pressure along with the formation of a high amount of nucleation germs allows to obtain particles smaller than those obtained in the other cases under study.

The results obtained on samples prepared by electrospinning were compared with those collected on samples synthesized by electrospray technique and by simple solvent evaporation at RT using TNBT precursor and thermal treatment in low oxygen pressure. The need of electrospinning technique for obtaining TiO_2 with very small crystallite size in anatase form was demonstrated. As a matter of fact, for samples obtained by electrospray and solvent evaporation the organic fraction was burn only at 650-700 °C, producing TiO_2 with high amount of rutile phase and crystallite size of about 20 nm.

References

[1] R. Bendoni, N. Sangiorgi, A. Sangiorgi, A. Sanson, Role of water in TiO2 screen-printing inks for dye-sensitized solar cells, Sol. Energy 122 (2015) 497-507.

[2] P. Yang, Q. Tang, A nanoporous titanium dioxide framework for dye-sensitized solar cell, Mater. Lett. 161 (2015) 185-188.

[3] T. Ochiai, S. Tago, M. Hayashi, H. Tawarayama, T. Hosoya, A. Fujishima, TiO_2-Impregnated porous silica tube and its application for compact air- and water-purification units, Catalysts 5(3) (2015) 1498-1506.

[4] M. Roso, A. Lorenzetti, C. Boaretti, D. Hrelja, M. Modesti, Graphene/TiO_2 based photo-catalysts on nanostructured membranes as a potential active filter media for methanol gas-phase degradation, Appl. Catal. B: Env. 176-177 (2015) 225-232.

[5] S.W. Verbruggen, TiO_2 photocatalysis for the degradation of pollutants in gas phase: From morphological design to plasmonic enhancement, J. Photochem. Photobio. C: Photochem. Rev. 24 (2015) 64-82.

[6] Z.-p. Yang, X. Liu, C.-j. Zhang, B.-z. Liu, A high-performance nonenzymatic piezoelectric sensor based on molecularly imprinted transparent TiO_2 film for detection of urea, Biosens. Bioelectron. 74 (2015) 85-90.

[7] W. Guo, Q. Feng, Y. Tao, L. Zheng, Z. Han, J. Ma, Systematic investigation on the gas-sensing performance of TiO_2 nanoplate sensors for enhanced detection on toxic gases, Mater. Res. Bulletin 73 (2016) 302-307.

[8] J. Moon, H.-P. Hedman, M. Kemell, A. Tuominen, R. Punkkinen, Hydrogen sensor of Pd-decorated tubular TiO_2 layer prepared by anodization with patterned electrodes on SiO_2/Si substrate, Sens. Actuators B: Chem. 222 (2016) 190-197.

[9] T. Amna, M.S. Hassan, W.-S. Shin, H. Van Ba, H.-K. Lee, M.-S. Khil, I.H. Hwang, TiO_2 nanorods via one-step electrospinning technique: A novel nanomatrix for mouse myoblasts adhesion and propagation, Colloids Surf. B: Biointerfaces 101 (2013) 424-429.

[10] S.J. Chen, H.Y. Yu, B.C. Yang, Bioactive TiO_2 fiber films prepared by electrospinning method, J. Biomed. Mater. Res. Part A 101A(1) (2013) 64-74.

[11] D. Li, Y.N. Xia, Fabrication of titania nanofibers by electrospinning, Nano Lett. 3(4) (2003) 555-560.

[12] G.M. Kim, S.M. Lee, G.H. Michler, H. Roggendorf, U. Goesele, M. Knez, Nanostructured pure anatase titania tubes replicated from electrospun polymer fiber templates by atomic layer deposition, Chem. Mater. 20(9) (2008) 3085-3091.

[13] R. Chandrasekar, L. Zhang, J.Y. Howe, N.E. Hedin, Y. Zhang, H. Fong, Fabrication and characterization of electrospun titania nanofibers, J. Mater. Sci. 44(5) (2009) 1198-1205.

[14] G. Li, J. Liu, G. Jiang, Facile synthesis of spiny mesoporous titania tubes with enhanced photocatalytic activity, Chem. Commun. 47(26) (2011) 7443-7445.

[15] G. He, Y. Cai, Y. Zhao, X. Wang, C. Lai, M. Xi, Z. Zhu, H. Fong, Electrospun anatase-phase TiO_2 nanofibers with different morphological structures and specific surface areas, J. Colloid Interface Sci. 398 (2013) 103-111.

[16] S. Sanwaria, S. Singh, A. Horechyy, P. Formanek, M. Stamm, R. Srivastava, B. Nandan, Fabrication of titania nanostructures using core–shell polymer nanofibers from block copolymers as templates, Nano-Structures & Nano-Objects 6 (2016) 14-22.

[17] A.G. MacDiarmid, W.E. Jones, I.D. Norris, J. Gao, A.T. Johnson, N.J. Pinto, J. Hone, B. Han, F.K. Ko, H. Okuzaki, M. Llaguno, Electrostatically-generated nanofibers of electronic polymers, Synth. Met. 119(1-3) (2001) 27-30.

[18] S.S. Choi, S.G. Lee, S.S. Im, S.H. Kim, Y.L. Joo, Silica nanofibers from electrospinning/sol-gel process, J. Mater. Sci. Lett. 22(12) (2003) 891-893.

[19] S.-H. Lee, C. Tekmen, W.M. Sigmund, Three-point bending of electrospun TiO_2 nanofibers, Mater. Sci. Eng. A 398(1â€“2) (2005) 77-81.

[20] W. Nuansing, S. Ninmuang, W. Jarernboon, S. Maensiri, S. Seraphin, Structural characterization and morphology of electrospun TiO_2 nanofibers, Mater. Sci. Eng. B 131(1-3) (2006) 147-155.

[21] S. Cavaliere, S. Subianto, I. Savych, D.J. Jones, J. Roziere, Electrospinning: designed architectures for energy conversion and storage devices, Energy Environ. Sci. 4(12) (2011) 4761-4785.

[22] G. He, X. Wang, M. Xi, F. Zheng, Z. Zhu, H. Fong, Fabrication and evaluation of dye-sensitized solar cells with photoanodes based on electrospun TiO_2 nanotubes, Mater. Lett. 106 (2013) 115-118.

[23] Y. Wen, B. Liu, W. Zeng, Y. Wang, Plasmonic photocatalysis properties of Au nanoparticles precipitated anatase/rutile mixed TiO_2 nanotubes, Nanoscale 5(20) (2013) 9739-9746.

[24] A. Yousef, N.A.M. Barakat, H.Y. Kim, Electrospun Cu-doped titania nanofibers for photocatalytic hydrolysis of ammonia borane, Appl. Catal. A: Gen. 467 (2013) 98-106.

[25] N.A.M. Barakat, E. Ahmed, M.A. Abdelkareem, A.A. Farghali, M.M. Nassar, M.H. El-Newehy, S.S. Al-Deyab, Ag, Zn and Cd-doped titanium oxide nanofibers as effective photocatalysts for hydrogen extraction from ammonium phosphates, J. Mol. Catal. A: Chem. 409 (2015) 117-126.

[26] A. Nikfarjam, N. Salehifar, Improvement in gas-sensing properties of TiO_2 nanofiber sensor by UV irradiation, Sens. Actuators B 211 (2015) 146-156.

[27] C. Peniche, D. Zaldivar, M. Pazos, S. Paz, A. Bulay, J.S. Roman, Study of the thermal degradation of poly(n-vinyl-2-pyrrolidone) by thermogravimetry-FTIR, J. Appl. Polym. Sci. 50(3) (1993) 485-493.

[28] W.K. Tang, W.K. Neill, J. Polym. Sci. 6 (1964) 65.

Figures and Captions

Figure 1 - SEM images of the as prepared samples obtained by electrospinning of solutions 2 (A), 4 (B), 5 (C) and 7 (D) with $TiOSO_4$ precursor. Instrumental magnification: 1000X.

Figure 2 - SEM images of the as prepared samples obtained by electrospinning of solutions 2 (A), 3 (B) and 5 (C) with TNBT precursor. Instrumental magnification: 1000X.

Figure 3 - TGA curves obtained with a temperature ramp of 10 °C/min for the samples prepared with solution 7 containing $TiOSO_4$ precursor (a) and solution 5 containing TNBT precursor (b).

Figure 4 - XRD patterns of TiOSair (a), TiOSOx (b), TNBTair (c) and TNBTOx (d).

Figure 5 - TEM (A) and HR-TEM (B) images of TNBTOx. Instrumental magnification: 50000X and 300000X, respectively. Inset C: Fourier Transform of the HR-TEM image in (B).

Figure 6 - Fiber diameter distribution (A) and particle size distribution (B) for TNBTOx sample. (n.f. = number of fibers; n.p. = number of particles).

Figure 7 - HR-TEM image of the TNBT sample before thermal treatment. Instrumental magnification: 250000X.

Figure 8 - SEM image of the as prepared sample obtained by electrospray of solution 5 with TNBT precursor and PVP of 30000 uma. Instrumental magnification: 5000X.

Figure 9 - XRD patterns of the TiO_2 samples obtained by electrospray (a) and by solvent evaporation (b).

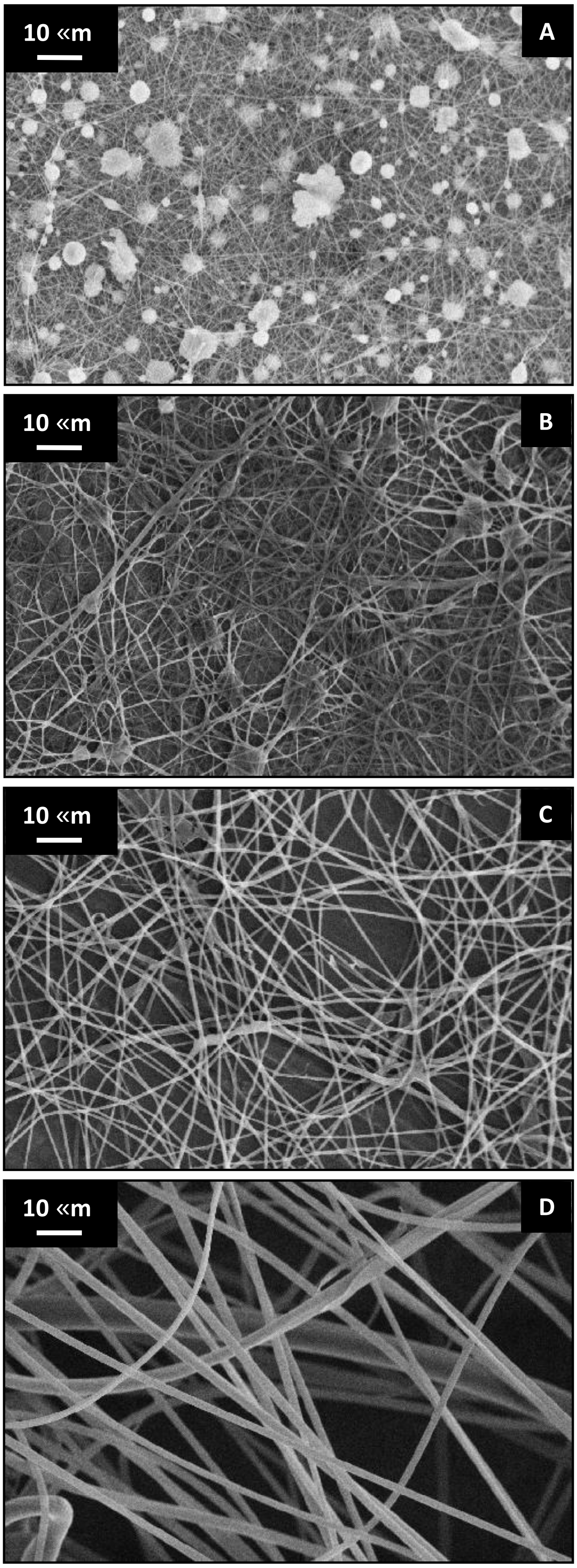

Figure 1

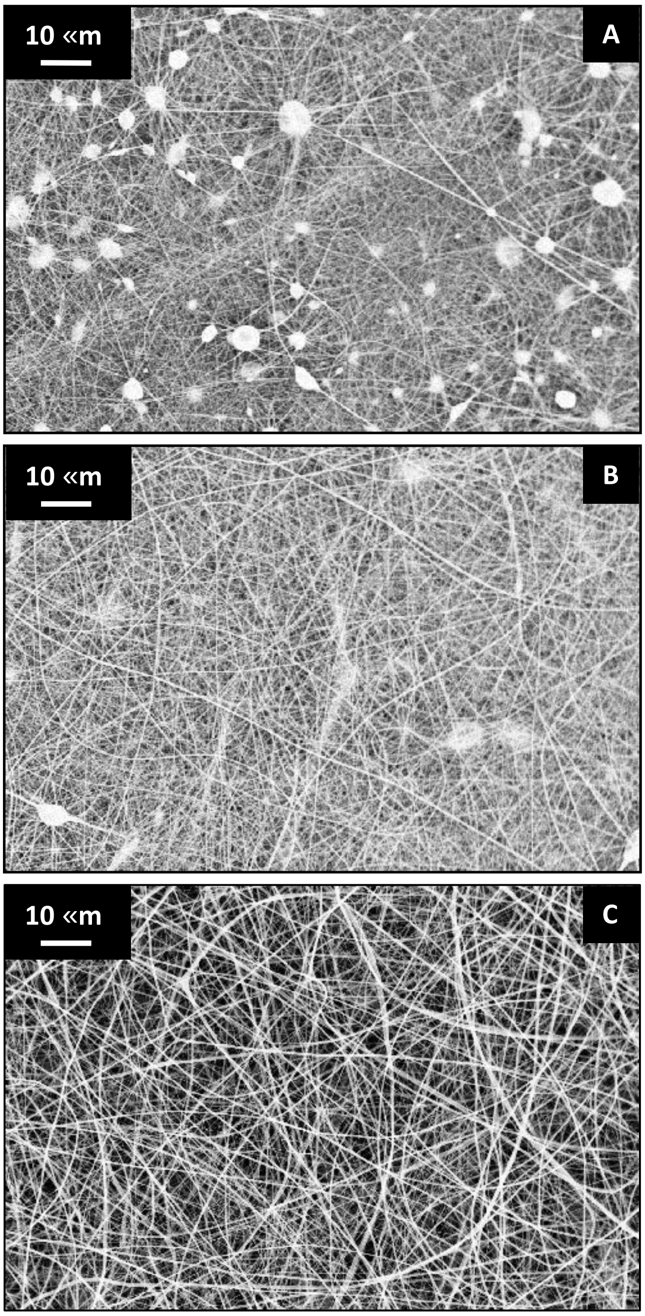

Figure 2

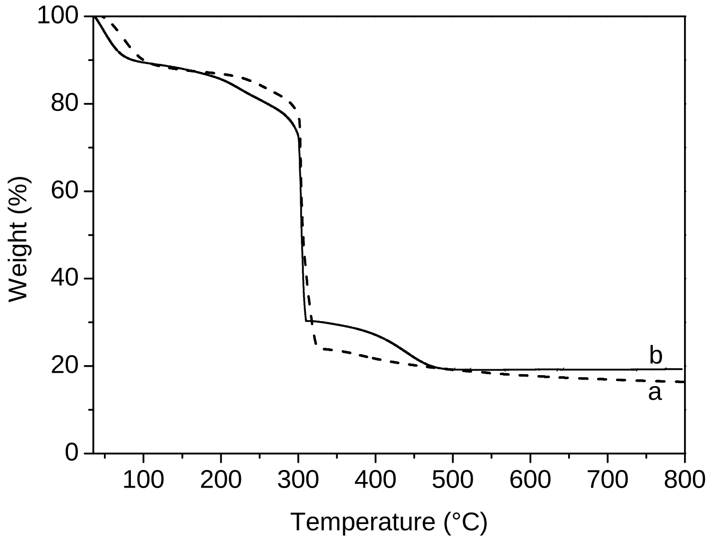
100
80
60
40
20
0
Weight (%)
100
200
300
400
500
600
700
800
Temperature (°C)
b
a

Figure 3

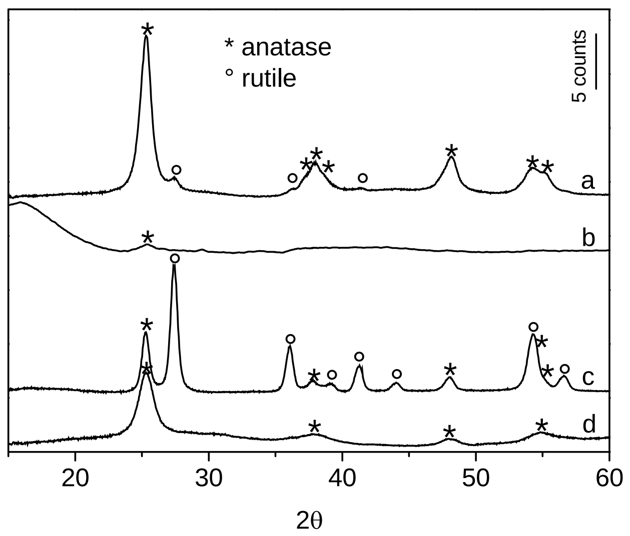

Figure 4

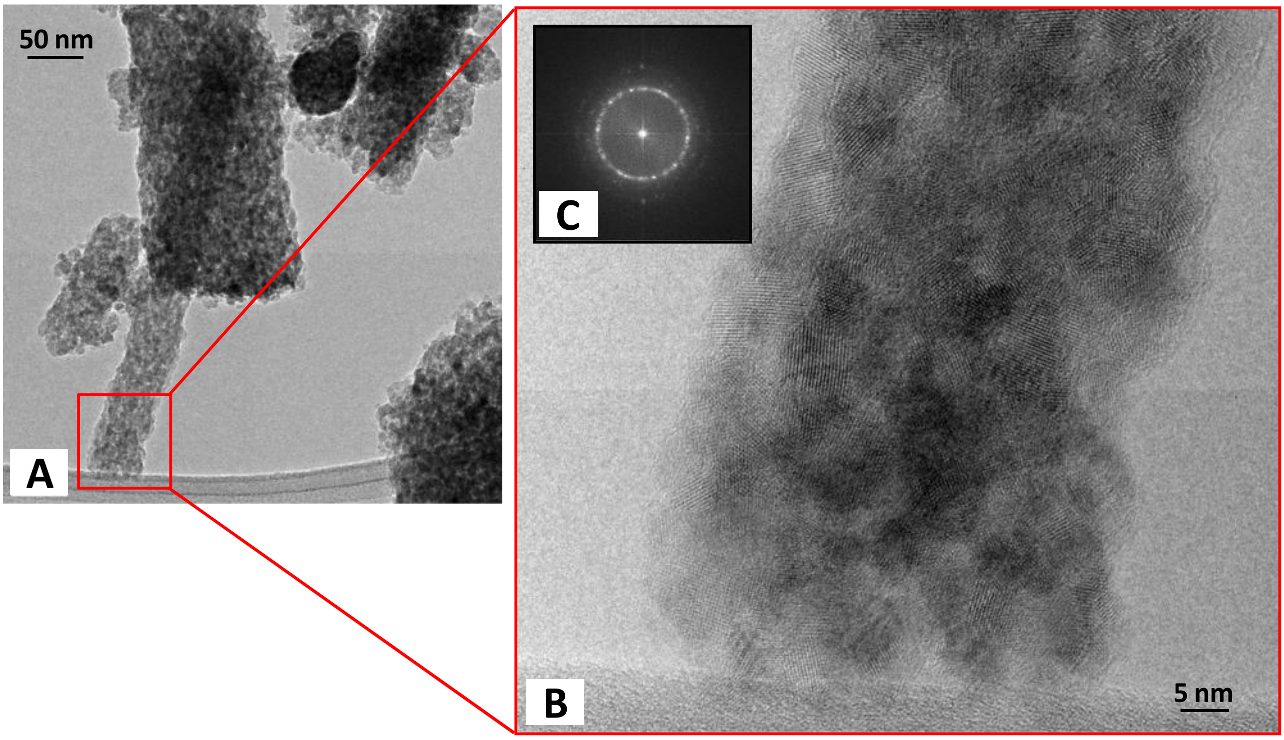

Figure 5

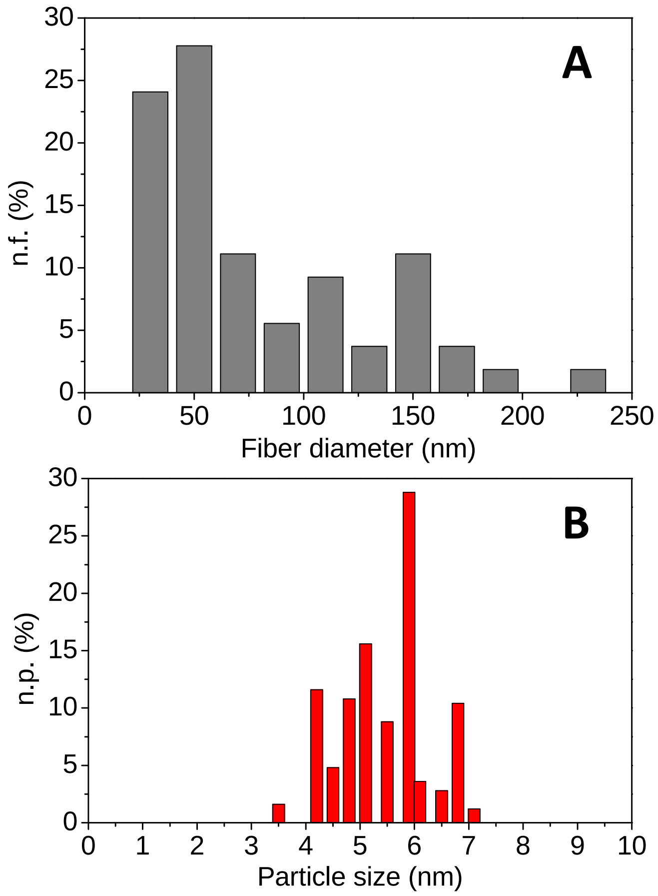

Figure 6

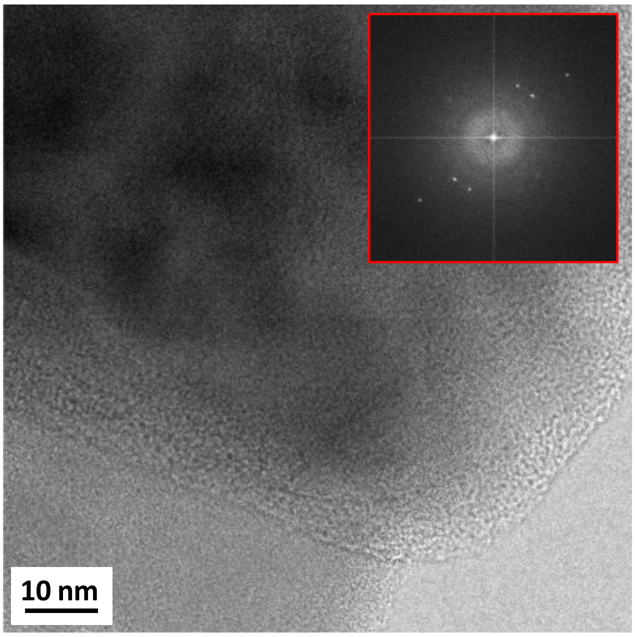

Figure 7

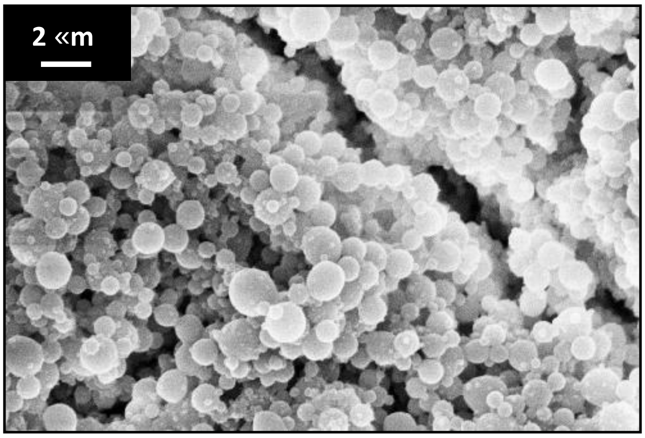

Figure 8

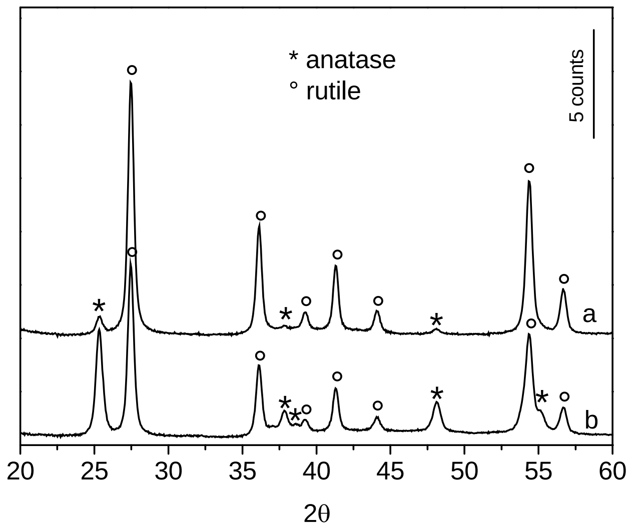

Figure 9